Available online at www.sciencedirect.com

SCIENCE DIRECT

Developmental Biology 279 (2005) 99–113

DEVELOPMENTAL BIOLOGY

www.elsevier.com/locate/ydbio

Dd-Alix, a conserved endosome-associated protein, controls *Dictyostelium* development

Sara Mattei[a], W. Jonathan Ryves[b], Béatrice Blot[c], Rémy Sadoul[c], Adrian J. Harwood[b], Michel Satre[a], Gérard Klein[a], Laurence Aubry[a,*]

[a]*The Laboratoire de Biochimie et Biophysique des Systèmes Intégrés (UMR 5092 CNRS-CEA-UJF), DRDC, CEA-Grenoble, 17 rue des Martyrs, 38054 Grenoble Cedex 9, France*

[b]*MRC Laboratory for Molecular Cell Biology, University College London, London WC1E 6BT, UK*

[c]*Laboratoire Neurodégénérescence et Plasticité (EMI 0108 INSERM-UJF), CHU-Grenoble -BP 217, 38043 Grenoble Cedex 9, France*

Received for publication 12 October 2004, revised 30 November 2004, accepted 3 December 2004
Available online 8 January 2005

Abstract

We have characterized the *Dictyostelium* homolog of the mammalian protein Alix. Dd-Alix is encoded by a single gene and is expressed during vegetative growth and multicellular development. We showed that the *alx* null strain fails to complete its developmental program. Past the tight aggregate stage, morphogenesis is impaired, leading to markedly aberrant structures containing vacuolated and undifferentiated cells but no mature spores. The developmental defect is cell-autonomous as most cells remain of the PstB type even when mixed with wild-type cells. Complementation analysis with different Alix constructs allowed the identification of a 101-residue stretch containing a coiled-coil domain essential for Alix function. In addition, we showed that the protein associates in part with vesicular structures and that its distribution on a Percoll gradient overlaps that of the endocytic marker Vamp7. Dd-Alix also co-localizes with Dd-Vps32. In view of our data, and given the role of Vps32 proteins in membrane protein sorting and multivesicular body formation in yeast and mammals, we hypothesize that the developmental defects of the *alx* null strain result from abnormal trafficking of cell-surface receptors.

Keywords: Alix; Development; Vps32; Endocytosis; *Dictyostelium*

Introduction

The protein Alix (ALG-2 Interacting protein X) has a widespread distribution in eukaryotes. Studies in several organisms initially suggested roles in a variety of biological processes. The first described member of the Alix family, Bro1, was identified in budding yeast as a genetic partner of the Pkc1p-MAP kinase pathway, which is activated in response to nutrient limitation. Deletion of *bro1* causes defects in cell wall integrity and cell shape abnormalities that are suppressed by overexpression of the BCK1 gene (MEKK) (Nickas and Yaffe, 1996). In mammals, Alix has been identified as a partner of the apoptosis-linked calciprotein ALG-2 (Apoptosis-Linked Gene 2) (Missotten et al., 1999; Vito et al., 1999) and of the SH3-containing protein SETA (SH3-containing protein Enhanced in Tumorigenic Astrocytes) found in tumorigenic astrocytes (Chen et al., 2000). These interactions suggested a possible link between Alix and cell death pathways, a hypothesis later supported both by evidence that human Alix is a negative regulator of cell transformation (Wu et al., 2002) and by the observation that overexpression of Alix C-terminus inhibits caspase-independent cell death (Trioulier et al., 2004). Recently, AIP-1/

Abbreviations: ESCRT, endosomal sorting complex required for transport; MVB, multivesicular body.

* Corresponding author. Fax: +33 438 786 107.
E-mail address: laubry@cea.fr (L. Aubry).

0012-1606/$ - see front matter © 2004 Elsevier Inc. All rights reserved.
doi:10.1016/j.ydbio.2004.12.004

Alix has also been shown to inhibit paraptosis, an alternative, nonapoptotic cell death program (Sperandio et al., 2004).

Consensus data in human and yeast with respect to a possible molecular function pertain to the association of Alix with the ESCRT (Endosomal Sorting Complex Required for Transport) machinery (Katoh et al., 2003; Odorizzi et al., 2003; Strack et al., 2003; Vincent et al., 2003; von Schwedler et al., 2003). The ESCRT complexes are involved in the formation of the multivesicular body (MVB). The MVB matures from early endosomes by invagination of intralumenal vesicles that carry, in their limiting membrane, cell surface transporters/receptors due to degradation (Katzmann et al., 2002). Deletion of bro1 or any member of the ESCRT complexes leads to an altered morphology of the MVB and a defect in the trafficking of membrane proteins originating from the Golgi or the plasma membrane (Katzmann et al., 2002; Luhtala and Odorizzi, 2004; Nikko et al., 2003; Springael et al., 2002). In mammals, the association of Alix with Tsg101/Vps23 and CHMP4/Vps32, components of ESCRT-I and ESCRT-III subcomplexes, has been demonstrated (Katoh et al., 2003; Strack et al., 2003; Vincent et al., 2003; von Schwedler et al., 2003) and a connection with trafficking has been suggested, via interactions with cytoskeletal elements and endophilins (Chatellard-Causse et al., 2002; Schmidt et al., 2003). Interestingly, Alix is selectively recruited onto liposomes containing lysobisphosphatidic acid, a phospholipid enriched in MVB, and strongly inhibits the formation of multivesicular liposomes (Matsuo et al., 2004). During the budding of retroviruses, a process topologically equivalent to MVB formation, Alix binds late-domain-containing viral proteins together with members of the ESCRT complexes (Strack et al., 2003; von Schwedler et al., 2003). By analogy, Alix may interact directly with target proteins en route to the MVB. Thus far, it is still a matter of debate as to whether the function of Alix in membrane protein trafficking accounts for the cell death observed under various conditions.

We chose to examine the role of Alix in *D. discoideum*, a multicellular organism described as a classical model for endocytic trafficking (Maniak, 2001) and more recently for programmed cell death (Golstein et al., 2003). In nutritive conditions, *Dictyostelium* multiplies as a unicellular organism that feeds on bacteria or by internalization of axenic medium by macropinocytosis. As nutrients are depleted, this organism ceases dividing and enters a multicellular developmental program, leading to a mature fruiting body comprising viable spores and stalk cells that die through a caspase/paracaspase-independent cell death process (Roisin-Bouffay et al., 2004). In this work, we generated an *alx* null mutant and analyzed the phenotypic consequences of the knockout. To get insight into how the protein functions, we investigated its subcellular distribution and documented its co-localization with the ESCRT protein homolog Dd-Vps32.

Materials and methods

Materials

Anti-myc 9E10 antibody was purchased from Roche Biochemicals (France). HRP-conjugated secondary antibodies were purchased from Biorad (France) and FITC- and Cy3-conjugated secondary antibodies from Jackson ImmunoResearch (USA). DAPI was obtained from Molecular Probes (France), DIF-1 from Affinity Research (UK) and Calcofluor from Sigma (France). The peptide corresponding to the putative GSK3 target region of Dd-Alix flanked by basic residues (RR-GVNPHSPLTSPSPS*LQSPV-RRR, where S* is phosphoserine) was synthesized by Zinsser Analytical Ltd. (UK). Purified recombinant GSK3β was purchased from New England Biolabs (USA).

Cloning

The sequence of the *Dictyostelium alx* gene was deposited at Genbank under accession number AF360741.

Plasmid constructs

The *alx*-derived overexpression constructs were made in pEXP4^{+} (neomycin resistance neo^{r}), using the *act15* promoter to control expression, except when mentioned otherwise. The full-length protein and deletion mutants were tagged at the C-terminus with a double myc epitope. The constructs are the following: Alix$_{myc2}$ (aa 1 to 794), AlixNt$_{myc2}$ (aa 1 to 596), AlixΔPro$_{myc2}$ (aa 1 to 697), AlixΔN1ΔPro$_{myc2}$ (aa 155 to 697), AlixΔN2ΔPro$_{myc2}$ (aa 293 to 697) and AlixCt$_{myc2}$ (aa 460 to 794). Point mutations within these constructs were generated by PCR, using mutated oligonucleotides. The *vps32* overexpression construct was made in DIPa (*act15* promoter, neomycin resistance neo^{r}). The *alx* gene disruption construct was generated by insertion of the THY1 cassette at position 927 bp of the cDNA, followed by a deletion of the next 13 bp. Recombinant forms of AlixCt and Dd-Vps32 (full-length) fused to the glutathione S-transferase (GST-AlixCt, GST-Vps32) were expressed in bacteria using the pGEX-KG vector. All the constructs that required PCR amplification steps were verified by sequencing.

Cell culture, development, and monolayer assay

Experiments were carried out with KAx-3 cells as the parental *D. discoideum* strain, except for the *alx* null mutant, which was made in the JH10 background, a thymidine auxotrophic strain derived from KAx-3. Cells were grown at 21°C in axenic medium in shaking

suspension or on plastic dishes. Knock-out thy$^+$ mutants were selected in axenic medium without addition of exogenous thymidine and cloned by plating cells onto SM-agar plates in association with *Klebsiella aerogenes*. The knock-out clones were checked by Southern and Western blot analyses. Mutant cells overexpressing various constructs were grown in suspension in HL5 medium containing G418 (20 μg/ml). Development of the mutants was monitored by plating cells on non-nutritive Na-KP$_i$-buffered agar plates containing 0.2 mM $CaCl_2$. Stalk cell induction by DIF was performed in a monolayer assay as described (Town et al., 1976).

Northern blot analysis

Cells were allowed to develop on Na-KP$_i$-buffered agar plates, harvested at the indicated times and the total RNA purified. Six micrograms of total RNA were separated on a formaldehyde-containing gel and transferred to a nitrocellulose membrane. The blot was probed with a DIG-labeled DNA fragment corresponding to full-length Dd-Alix.

Production of antibodies and Western blot analysis

The rabbit polyclonal anti-Alix and anti-Vps32 antibodies were raised against the C-terminal domain of Dd-Alix and the full-length Dd-Vps32, both expressed as a fusion protein with GST (GST-AlixCt and GST-Vps32). The GST-fused proteins expressed in Bl21-DE3 (3 h at 37°C, 1 mM IPTG) were purified from the inclusion bodies according to a published procedure (Harlow and Lane, 1988) and used to immunize New Zealand White rabbits. The 81-day sera were used at a 1/1000 dilution for Western blot analysis. The proteins were detected by enhanced chemiluminescence (ECL). Alternatively, the myc-tagged proteins were followed using the anti-myc antibody (5 μg/ml). Anti-VAMP7 serum was used at a 1/200 dilution.

Cell-type labeling

Cells carrying the constructs *act15/lacZ*, *SP60/lacZ*, and *ecmA/lacZ* were allowed to develop on nitrocellulose filters laid on non-nutritive agar plates and subjected to β-galactosidase staining. Cell staining was performed as described earlier (Haberstroh and Firtel 1990; Mann et al. 1994). Cells carrying the constructs *alx/gfp*, *act15/gfp*, and *ecmB/gfp* were plated on non-nutritive agar-plates and observed directly as development proceeded on a Nikon SMZU stereoscopic microscope equipped with a fluorescence attachment and a GFP filter. Calcofluor cellulose staining was performed as described (Harrington and Raper, 1968).

Immunofluorescence

Except when mentioned, cells were allowed to adhere onto 8-well Labtek slides for 20 min. Immunostaining was then performed as described (Aubry et al., 2002). Primary antibodies were used at 5 μg/ml for the anti-myc antibody 9E10 or at a 1/400 dilution for anti-Alix and anti-Vps32 antibodies. After extensive washes, cells were incubated with FITC- or Cy3-conjugated goat anti-mouse or anti-rabbit antibodies for 1 h. After further washing steps, cells were mounted and visualized on a Zeiss Axiovert 200 M microscope. For starved cell staining, cells were let to aggregate overnight on the slide of the Labtek chamber in non-nutritive buffer prior to fixation. Whole-mount immunostaining was performed on slugs overexpressing Alix$_{myc2}$ as published (Jermyn et al., 1989).

Subcellular fractionation

Cells were broken with 0.17 mm glass beads in buffer made of 40 mM MES-Na, pH 6.0, 1 mM EDTA and 0.25 M sucrose (MESES buffer) containing a protease inhibitor cocktail. Membranes and cytosol were separated by a 30-min centrifugation at 13,000 × g. The pellet was resuspended in the initial volume of breaking buffer containing, when indicated, 1% Triton X-100. Treated membranes were recovered by centrifugation at 100,000 × g and the pellet resuspended in the initial volume of buffer. Final membrane and soluble fractions were analyzed by denaturing polyacrylamide electrophoresis.

Gradient analysis

Cells (1.5×10^9), either in vegetative phase or developed for 6 h on Na-KP$_i$ buffered agar plates, were broken in MESES buffer plus protease inhibitors and the post-nuclear supernatant (3 ml) fractionated on a self-forming 24% Percoll gradient in the same buffer as described earlier (Aubry et al., 2002). The gradient was eluted from the bottom of the tube. Acid phosphatase activity was determined using p-nitrophenyl phosphate as a substrate. Proteins of interest were detected by Western blot analysis.

Biotinylation assay

Prior to biotinylation, vegetative cells were washed and pulsed every 6 min with 30 nM pulses of cAMP in 12 mM Na-KP$_i$ buffer, pH 6.5 over a period of 4 h to mimic aggregation. Cells were then stimulated by addition of 300 μM cAMP every 2 h to induce differentiation. At indicated times, 10^7 cells were harvested, washed once in 17 mM Na-KP$_i$ buffer, pH 8.0 plus 120 mM sorbitol and resuspended in 2 ml of the same buffer containing or not 1 mg/ml sulfo-NHS-LC biotin. Cells were incubated on ice for 15 min with occasional mixing. Biotinylation was stopped by washes in 100 mM glycine, pH 8.0. Cells were then resuspended in Laemmli buffer. Biotinylation efficiency was estimated by Western blot analysis using streptavidin-HRP (0.5 μg/ml).

GSK3 kinase assay

GSK3-specific activity was determined as described previously (Ryves et al., 1998) using the synthetic Alix peptide as substrate. Assays were conducted in duplicate and calculations were performed after subtraction of the baseline activity. Michaelis constant (K_m) for the Alix peptide was determined from the direct plots of velocity and peptide concentrations and from the double reciprocal plots (Lineweaver-Burke representation).

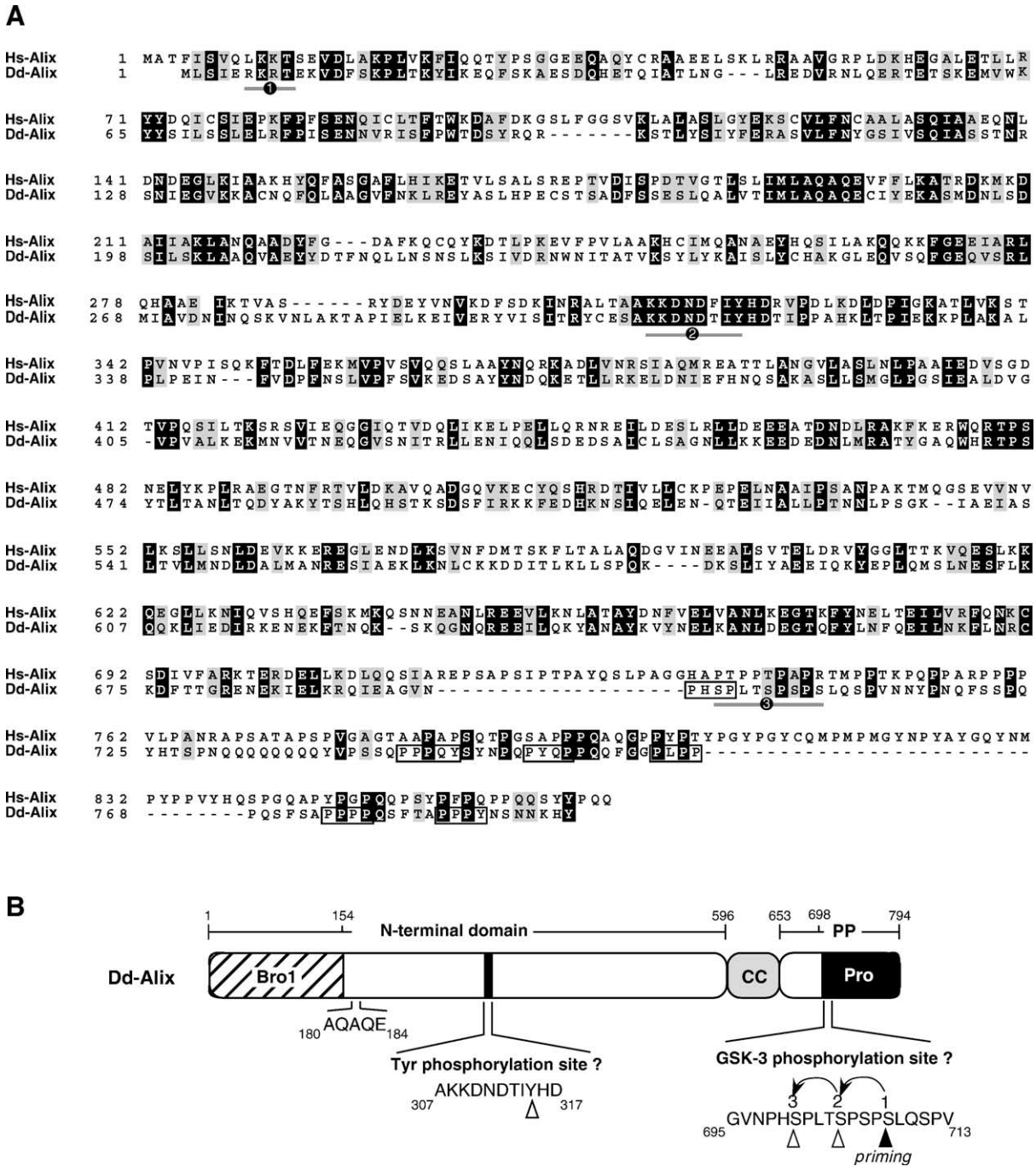

Fig. 1. Alignment of *Dictyostelium* and human Alix proteins and schematic domain representation. (A) An amino-acid alignment was generated using the Clustal W program (Thompson et al., 1994) with the *Dictyostelium* and human Alix sequences. Identities and homologies are boxed with black or grey shading, respectively. Putative phosphorylation sites by protein kinase A (1), tyrosine kinase (2) and GSK3 (3) are underlined. SH3-binding and WW-binding sequences are boxed. (B) Schematic representation of the domain structure of Alix from *Dictyostelium*. The relevant domains are schematized: the Bro1 domain included in the N-terminal domain, the coiled-coil domain (CC) and the proline-rich region (Pro) that is included in a larger region referred to as PP. The conserved AQAQE sequence and the putative tyrosine- and GSK3 phosphorylation sites are highlighted. The priming serine in the GSK3 site (site 1) is indicated by a black triangle. Open triangles mark residues that are potentially phosphorylated in the GSK3 and the tyrosine kinase sites.

Results

The Dictyostelium genome contains a homolog of human Alix

The *Dictyostelium* database was searched using the BLAST 2.0 algorithm for a homolog of mammalian Alix. Several clones corresponding to partial sequences were found. The full-length genomic sequence of the *Dictyostelium alx* gene was determined by PCR and the coding sequence obtained by RT-PCR. The *alx* gene consists of 4 exons and 3 short (95, 109 and 205 bp) AT-rich introns at positions 247, 783 and 1365 of the genomic DNA. *Dictyostelium alx* gene is localized on chromosome 2 (Glöckner et al., 2002). This gene encodes a 794-amino acid-long Dd-Alix protein with calculated Mr of 90.5 kDa and pI of 6.3. Alignment of the entire protein with mouse, human and frog homologs gave ~30% sequence identity. Highest homology (40% identity and 60% similarity) was present in the N-terminal region, which contains the Bro1 signature named after the yeast homolog (PfamA domain 03097). The amino acid alignment of Alix from *Dictyostelium* and human (Fig. 1A) revealed additional highly conserved sequence motifs. They included a putative protein kinase A phosphorylation site at the N-terminal extremity, the sequence AQAQE of unknown function at position 180 (numbering based on the *Dictyostelium* sequence) and a consensus tyrosine phosphorylation sequence KKDN-DTIY at position 308. Other structural characteristics of Dd-Alix also shared with Alix orthologs were a helical region predicted to form a coiled-coil (aa 600 to 653) and a C-terminus rich in proline residues that was organized into several putative SH3- and WW-binding motifs (Fig. 1B). This polyproline region in vertebrate Alix contains an ALG-2 binding domain (Trioulier et al., 2004), a SETA binding site (Chen et al., 2000) and an endophilin-binding sequence PxRPPPP (Chatellard-Causse et al., 2002). Unusual features of Dd-Alix were the presence of a pseudo-repeat PQSFSAPPP-PQSFTAPPP close to the C-terminus and a potential double phosphorylation site for the serine-threonine kinase GSK3 at position 700–708 (SPLTSPSPS, Fig. 1B) that revealed to be a good substrate when tested as a peptide in vitro (K_m values 2.3–2.7 μM).

Dd-Alix is expressed throughout development

Under nutritive conditions, *D. discoideum* grows as a unicellular organism. In response to starvation, *Dictyostelium* enters a program of multicellular development, the first stages of which involve aggregation of individual cells to form a mound (Aubry and Firtel, 1999). The outcome of this 24-h process is the fruiting body, in which about 80% of the cells form encapsulated spores. The remaining cells differentiate mainly into dead stalk cells and are patterned to produce the morphology of the fruiting body. Differentiation and patterning of the fruiting body begin at the mound stage (8 h) with the induction of precursor cell types, the prestalk and prespore cells (Williams et al., 1989). Expression of Dd-Alix along the developmental program was followed by Northern and Western blotting. Dd-Alix mRNA was present throughout development, with a slightly higher level in vegetative cells and during early development (Fig. 2A). For Western blot analysis, a polyclonal anti-Alix antibody was raised against the C-terminal domain (aa 460 to 794) of Dd-Alix. Its specificity was validated on the *alx* knock-out strain (see below) as illustrated (Fig. 2B). An almost constant level of expression, with a slight decrease towards the end of culmination, was observed at the protein level (Fig. 2C). Such a pattern of expression is consistent with the participation of Dd-Alix in a general cellular function during the developmental cycle.

Dd-Alix disruption leads to a developmental defect

To investigate the function of Dd-Alix, a knock-out strain was constructed by homologous recombination and verified

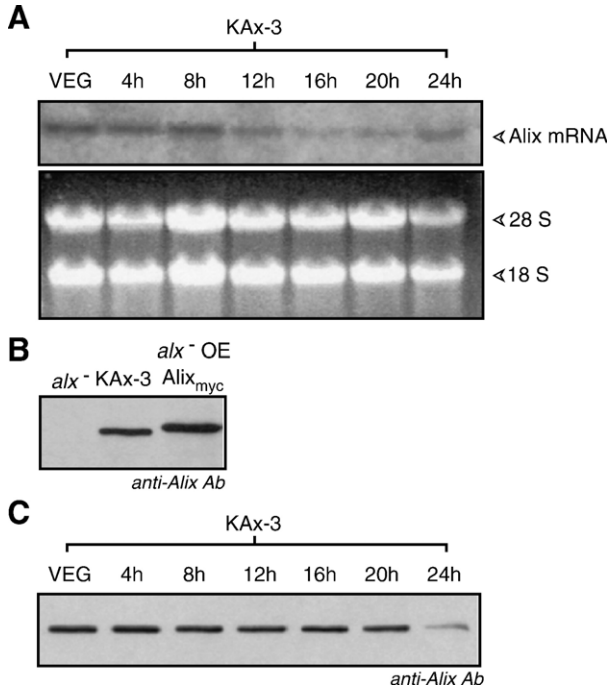

Fig. 2. Expression of Dd-Alix along development and validation of *alx* knock-out strain. (A) A Northern blot analysis was performed on total RNA prepared from KAx-3 amoebae at different times of development (every 4 h over a 24-h period). The membrane was probed with a DIG-labeled DNA probe directed against the entire Dd-Alix sequence (top panel). Equivalent loading on the gel and transfer to the membrane was controlled by staining ribosomal RNAs with ethidium bromide (bottom panel). (B) Protein extracts from KAx-3, *alx* null and *alx* null expressing Alix$_{myc2}$ cells from vegetative stage were probed with the anti-Alix antibody as a control of *alx* deletion, antibody specificity and overexpression level. The same amount of proteins was loaded in each lane. (C) Temporal expression of endogenous Dd-Alix was followed as a function of time during development. Whole-cell protein extracts were separated on an 8% SDS-gel, transferred to Immobilon-P membranes and probed with a 1/1000 dilution of the anti-Alix serum. Proteins were detected using the ECL technique.

by Southern blot (unpublished data) and Western blot (see Fig. 2B). In nutritive conditions, the *alx* null strain grew normally either on bacteria or in axenic medium. The mutant displayed no obvious defect in macropinocytic activity, as followed by internalization of FITC-dextran (unpublished data). Under nutrient deprivation, however, the null strain exhibited a major defect in development. Cells aggregated with normal timing but, past the tight aggregate stage, morphogenesis was severely impaired and gave rise to aberrant finger structures (Fig. 3A, compare the wild-type KAx-3 strain in lower panel to the null mutant in top panel). The majority of aggregates arrested development at this stage, although very occasionally, some gave rise to small fruiting bodies after extended periods of development.

The morphology of the cells forming the terminal, pseudo-finger structure was observed at high magnification to check for the presence of ovoid spores or vacuolated stalk cells. The multicellular *alx* null organism comprised mainly two populations of cells, undifferentiated cells (Und) and large sized cells (Vac), most of which harbored one or more large intracellular vacuoles, whose morphology was reminiscent of that of the parental stalk cells (Fig. 3A). The vacuolated cells were positively stained with Calcofluor, a specific marker for cellulose (Fig. 3B). No cells with the appearance of spores were observed. Dd-Alix is therefore essential for completion of the developmental cycle. To confirm the ability of the *alx* null cells to differentiate stalk cells, the mutant cells were developed in monolayers in the presence of the appropriate morphogens, cAMP and the differentiation-inducing factor DIF-1, under conditions described to induce the differentiation into stalk cells (Kay and Jermyn, 1983). After such treatment, *alx* null cells formed vacuolated stalk cells, as observed for the parental strain (Fig. 3C).

Dd-Alix is required for cell-type differentiation

To further characterize the defects linked to the *alx* null mutation, and to define the impaired developmental step, we examined the effect of *alx* deletion on the differentiation of the precursor cells and their patterning within the multicellular organism. The prestalk-specific *ecmA*, *ecmB*, and prespore-specific *SP60* were used as markers of normal development. Northern blot analysis detected very low

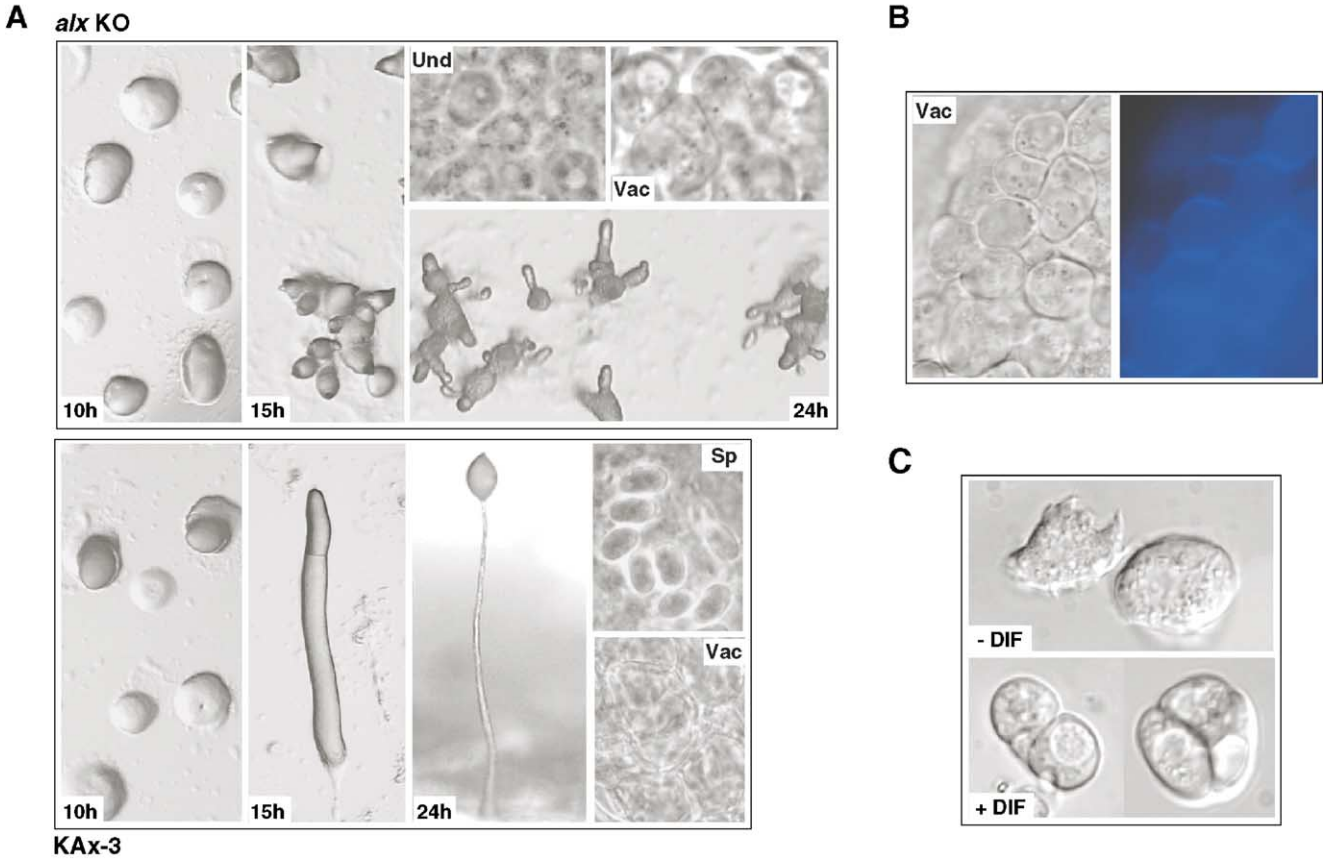

Fig. 3. Developmental phenotypes of alx null mutant and KAx-3. (A) KAx-3 and *alx* null cells were let to develop on non-nutritive agar plates. The developmental phenotypes observed at stages 10, 15, and 24 h are illustrated. After 24 h of development, cells forming the multicellular structure were observed at higher magnification. In KAx-3, spore (Sp) and vacuolated (Vac) stalk cells could be observed, whereas the *alx* null strain was mostly composed of undifferentiated (Und) cells and vacuolated (Vac) cells. (B) The vacuolated cells from the *alx* null structure were stained with Calcofluor. (C) The ability of *alx* null cells to differentiate stalk cells was tested in monolayer assay. Cells were sequentially submitted to cAMP and DIF and observed after 24 h for vacuolation. All photographs were taken on a Nikon SMZ-U dissecting microscope equipped with a Sony 3CCD color video camera.

levels of the predifferentiation markers ecmA and SP60 (data not shown). This result was confirmed by the use of reporter constructs consisting of the cell-type specific promoter of *ecmA*, *ecmB* and *SP60* genes fused to reporter genes (β-galactosidase or GFP). In KAx-3 cells, the prestalk cells, initially scattered within the aggregate, sorted to the tip of the mound to eventually form the anterior region of the first finger. The prespore cell population (SP60-positive) occupied the rest (80%) of the multicellular structure. In the mound formed by *alx* null cells, *ecmA*- or *SP60*-dependent staining was barely visible (Fig. 4A). Many ecmB-positive cells were present within the mound. After a longer period of development, giving rise to the final pseudo-fingers in the *alx* null mutant, the prespore-specific construct was slightly induced at the tip of the structure, as shown by the faint blue color of the cells comprising the tip. The rest of the organism was moderately stained with the prestalk-specific construct *ecmA/lacZ* and was also strongly ecmB-positive. The fact that most cells were able to activate *ecmB* promoter at a high level, and this before they could induce *ecmA* promoter, is reminiscent of the behavior of the PstB cell population.

The alx null defect is cell-autonomous

We next analyzed the behavior of the knock-out mutant in mixtures with the *Dictyostelium* wild-type strain KAx-3 to examine possible cooperative interactions between the two strains. This approach was aimed at revealing the cell autonomy of the defect due to *alx* knock-out. *alx* null cells, expressing either *act15/lacZ* or *act15/gfp* constructs, were mixed at a ratio of 1:3 with the wild-type strain and allowed to develop multicellular structures (Fig. 4B). At the mound stage, the null mutant exhibited a homogeneously scattered pattern in the chimeras, indicating a participation in development equivalent to the wild-type strain. At the slug stage, however, most of the stained cells were restricted to the extreme posterior of the slug and some of them were left behind as the slug migrated. Once the fruiting body was formed, only a very few null cells were found in the spore mass, indicating that the presence of the wild-type cells failed to rescue the defect of the *alx* null mutant regarding prespore differentiation (cell autonomous defect). The majority of the stained cells were located in the lower part of the stalk of the fruiting body. Some cells were also visible in the lower cup and to a lesser extent in the upper cup. They were excluded from the stalk and the stalk tube. The use of cell-type-specific constructs to label the null strain revealed that most cells found at the rear of the slug and at the base of the fruiting body were ecmB- and ecmA-positive, a behavior expected for PstB cells. The PstB population usually represents less than 10% of the whole differentiating population (Early et al., 1995). In the *alx* null mutant, the expansion of the PstB population is at the expense of the prespore population. As hardly any SP60-positive cells were detected within the *alx* null aggregate, it is unlikely that an established prespore population transdifferentiated into prestalk cells. Our data thus suggest a model in which deletion of *alx* inhibits the prespore differentiation pathway and favors the PstB-fate pathway. Noticeably, the PstB-like cells issuing from the *alx* null population remained clustered on top of the parental basal disc in the chimeric organism (Fig. 4B).

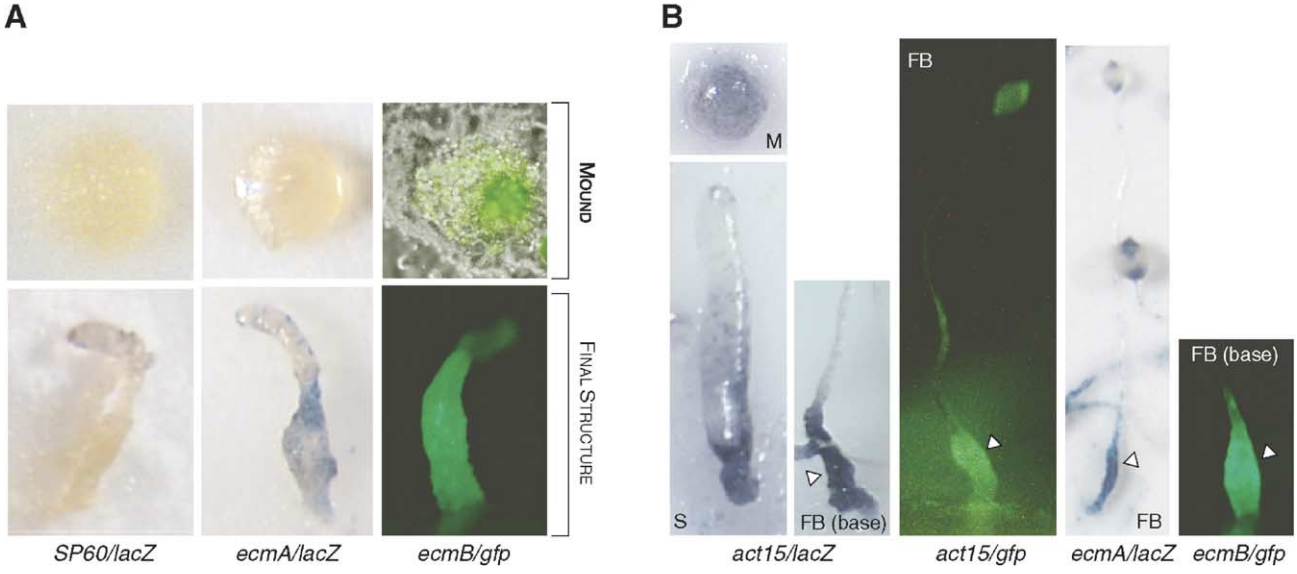

Fig. 4. Expression of cell-type specific markers in *alx* null cells and behavior in chimeras. (A) *alx* null cells carrying the reporter constructs *SP60/lacZ*, *ecmA/lacZ* or *ecmB/gfp* were allowed to develop to the mound stage or to the final structure. Aggregates were histochemically stained for β-galactosidase activity or directly observed for their fluorescence as described in Materials and methods. (B) *alx* null cells carrying the reporter constructs *act15/lacZ*, *ecmA/lacZ*, or *ecmB/gfp* were allowed to co-aggregate with parental cells in a 1:3 ratio and form chimeric organisms. Structures were stained (lacZ) or directly observed (GFP) as above, at mound (M), slug (S), or fruiting body (FB) stages.

The Dd-Alix domains are differentially required for its functional role

Alix is a multimodular protein. To gain functional insight into the role of Dd-Alix subdomains, several truncated forms of Alix were engineered and expressed in *alx* null cells to test their ability to complement the developmental defect: Alix, AlixCt, AlixNt, AlixΔPro, AlixΔN1ΔPro, and AlixΔN2ΔPro (Fig. 5A). The constructs are presented in Table 1). Considering the temporal pattern of expression of Dd-Alix (Fig. 2C), the constitutive *act15* promoter was used to direct the expression of the various cDNAs. A double myc epitope was also introduced at the C-terminus to follow expression of all the constructs. The presence of the recombinant proteins was first ascertained by Western blot. Surprisingly, whereas all the tested constructs were expressed at detectable levels (close to the endogenous level, Fig. 2B) in vegetative cells, $AlixCt_{myc2}$, $AlixΔN1ΔPro_{myc2}$, and $AlixΔN2ΔPro_{myc2}$ proteins were completely absent from developed protein extracts (Fig. 5B, Table 1). These three constructs all lack the Bro1 domain. The exact reason for this instability is not known, but the data suggest that loss of this specific region renders the truncated protein more sensitive to a yet uncharacterized, developmentally regulated degradation event. As expected from this loss of expression, these constructs failed to complement the developmental defect of the null strain and could not be used to evaluate the contribution of the N-terminal domain to the function of Dd-Alix. Overexpression of $Alix_{myc2}$ in *alx* null cells fully restored the parental phenotype, with formation of normal-looking fruiting bodies, as anticipated for a phenotype strictly due to *alx* disruption (Fig. 5B). Interestingly, a construct deleted of its proline-rich C-

Table 1
Expression and ability to complement the *alx* null developmental phenotype of the mutated and truncated Dd-Alix constructs

Constructs	Expression during development	Complementation of *alx* null strain
Alix	+	+
$Alix^{Q181E/Q183E}$	+	+
$Alix^{D310A/N311A}$	+	+
$Alix^{Y315D}$	+	+
$Alix^{Y315F}$	+	+
$Alix^{S700A/S704A/S708A}$	+	+
$Alix^{S700D/S704D/S708D}$	+	+
AlixΔPro[a]	+	+
AlixNt[b]	+	–
AlixΔN1ΔPro[c]	–	–
AlixΔN2ΔPro[d]	–	–
AlixCt[e]	–	–

[a] aa 1–697.
[b] aa 1–596.
[c] aa 155–697.
[d] aa 293–697.
[e] aa 460–794.

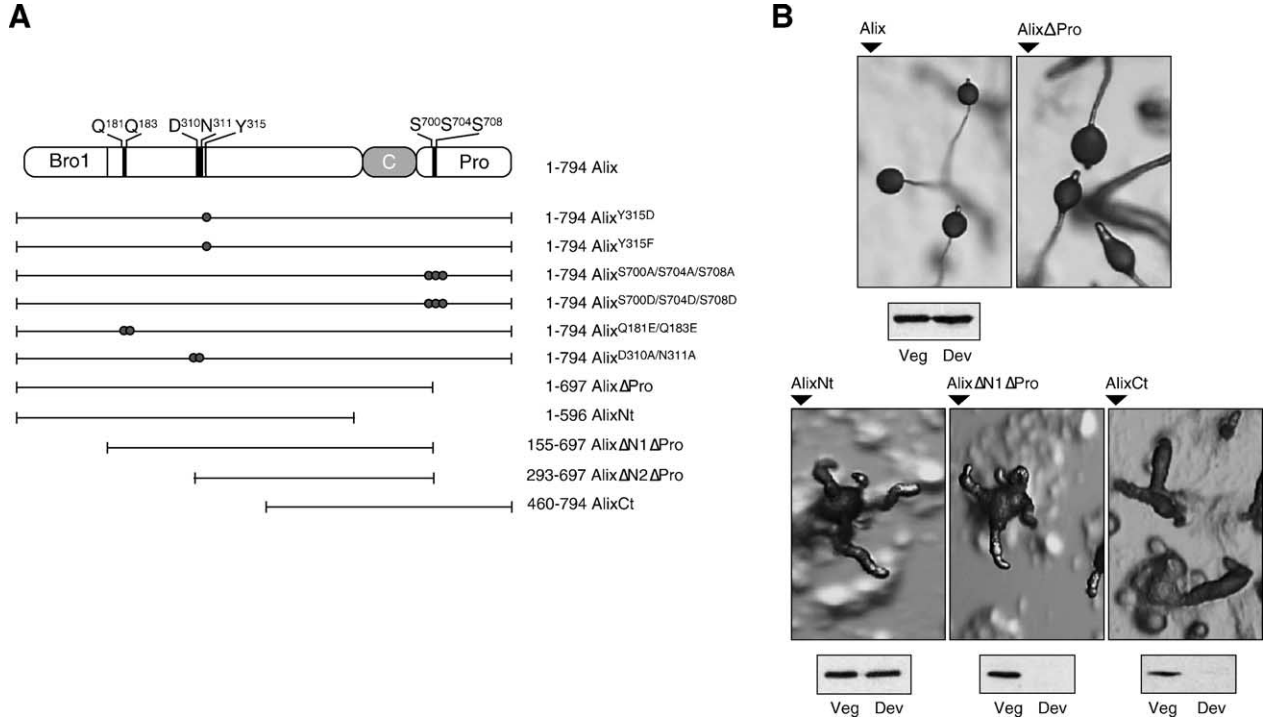

Fig. 5. Complementation of the *alx* null phenotype. *alx* null cells were transformed with various myc-tagged constructs summarized in panel A in order to test their ability to complement the null developmental phenotype. (B) Cells were plated on non-nutritive agar plates and let to develop for 30 h. The pictures represent the final developmental phenotype of selected mutants. Cells were also harvested in vegetative conditions and at mound stage to check the expression of the constructs. A whole protein extract from each mutant (act15/alx_{myc2}, act15/$alxNt_{myc2}$, act15/$alxΔN1ΔPro_{myc2}$, act15/$AlixCt_{myc2}$) was analyzed by Western blot with the anti-Alix antibody.

terminal domain was still able to complement the developmental defect of *alx* null mutant, as attested by the presence of fruiting bodies (Fig. 5B). These results demonstrate that the proline-rich C-terminal domain site is dispensable for complementation. Further deletion into the C-terminal domain, removing the putative coiled-coil domain ($AlixNt_{myc2}$), generated a truncated protein which was unable to complement, despite a suitable level of expression during development, thus defining a 101-amino acid region (position 597–697) essential for Alix function (Table 1, Fig. 5B).

In addition to its overall domain organization, Dd-Alix shares with its counterparts from fungi or higher eukaryotes several conserved motives, including a highly conserved AQAQE sequence and a consensus tyrosine phosphorylation sequence KKDNDTIY that may regulate the kinetics of Alix activity (Fig. 1). To evaluate the role of these supposedly critical amino acid stretches, the *alx* null strain was transformed with different constructs carrying the following mutations: Q181E/Q183E, Y315D, mimicking a constitutive phosphorylation, Y315F mimicking a non-phosphorylated state, and D310A/N311A likely to interfere with phosphorylation of Y315. All constructs were able to complement the differentiation defect of the *alx* null cells (Fig. 5A, Table 1) suggesting that none of these amino acids are essential for Alix functioning during development.

We showed above that deletion of the PRD that includes the in vitro tested GSK3 phosphorylation sites yields a protein functional enough to complement the null strain. If GSK3 functions as a negative regulator of Alix activity, deletion of the whole PRD domain could mask such type of regulation. We therefore specifically tested the role of GSK3 by mutating the serine residues of the target site into alanines or aspartic acids, the latter being expected to mimic a constitutively phosphorylated substrate. None of these substitutions altered the ability of Alix to complement the null defect (Fig. 5A, Table 1).

Dd-Alix associates with endosomal membranes

We next analyzed the subcellular distribution of Dd-Alix during growth and development to approach Alix function. The localization was first investigated by immunocytochemistry. The anti-Alix antibody was validated as Alix-specific by the absence of immunostaining in the *alx* null cells. In vegetative KAx-3 cells, the signal was faint but some Alix was detectable within the cytosol and also on scattered small sized vesicular structures (unpublished data). A similar but stronger staining was obtained in the *alx* null strain expressing $Alix_{myc2}$ under the *act15* constitutive promoter using either anti-Alix (unpublished data) or anti-myc antibodies (Fig. 6, Veg). In view of the low level of $Alix_{myc2}$ overexpression in this strain (Fig. 2B, at most twice the endogenous level) in addition to its ability to complement the null strain phenotype, it was reasonable to think that the behavior of $Alix_{myc2}$ reflected that of the endogenous protein. Thus, subsequent immunofluorescence analyses were performed on this strain. In cells starved for several hours in non-nutritive phosphate buffer, $Alix_{myc2}$ immunostaining still displayed a punctate pattern. However, vesicles appeared more distinctly on the cytosolic background and of a larger size than in vegetative cells (Fig. 6, Agg). A similar distribution was observed in slugs subjected to whole-mount immunofluorescence (Fig. 6, Slug).

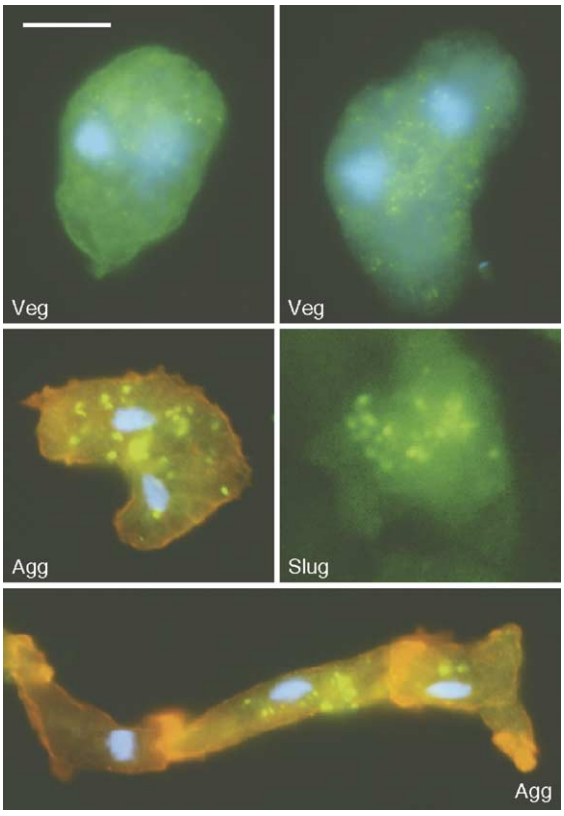

Fig. 6. Intracellular localization of Dd-Alix. *alx* null cells expressing $Alix_{myc2}$ under a constitutive *act15* promoter were fixed as mentioned in Materials and methods at various stages of development. The myc tag was detected with an anti-myc antibody followed by a goat anti-mouse FITC-coupled secondary antibody. Nuclear staining was performed with DAPI. In aggregating cells, F-actin was stained with TRITC-phalloidin. Veg: vegetative cells, Agg: starved cells streaming to form mounds, Slug: slug cells. Photographs were made on the Zeiss Axiovert 200M microscope equipped with a black and white Axiocam model camera using the Axiovision software. Staining is presented with false colors. Scale bars represent 5 μm.

To characterize the nature of the Alix-positive compartments, we followed the distribution of endogenous Dd-Alix after subcellular fractionation of a post-nuclear supernatant from vegetative cells on a Percoll gradient (Fig. 7A). Dd-Alix partitioned between the soluble top fractions and deeper fractions of the gradient as expected from the immunofluorescence data. Most of Dd-Alix co-localized in fractions 8 to 11 with the endosomal protein VAMP7 and the endocytic hydrolase acid phosphatase, therefore suggesting an endosomal association of Dd-Alix. However, Dd-Alix was essentially excluded from the lysosomal compart-

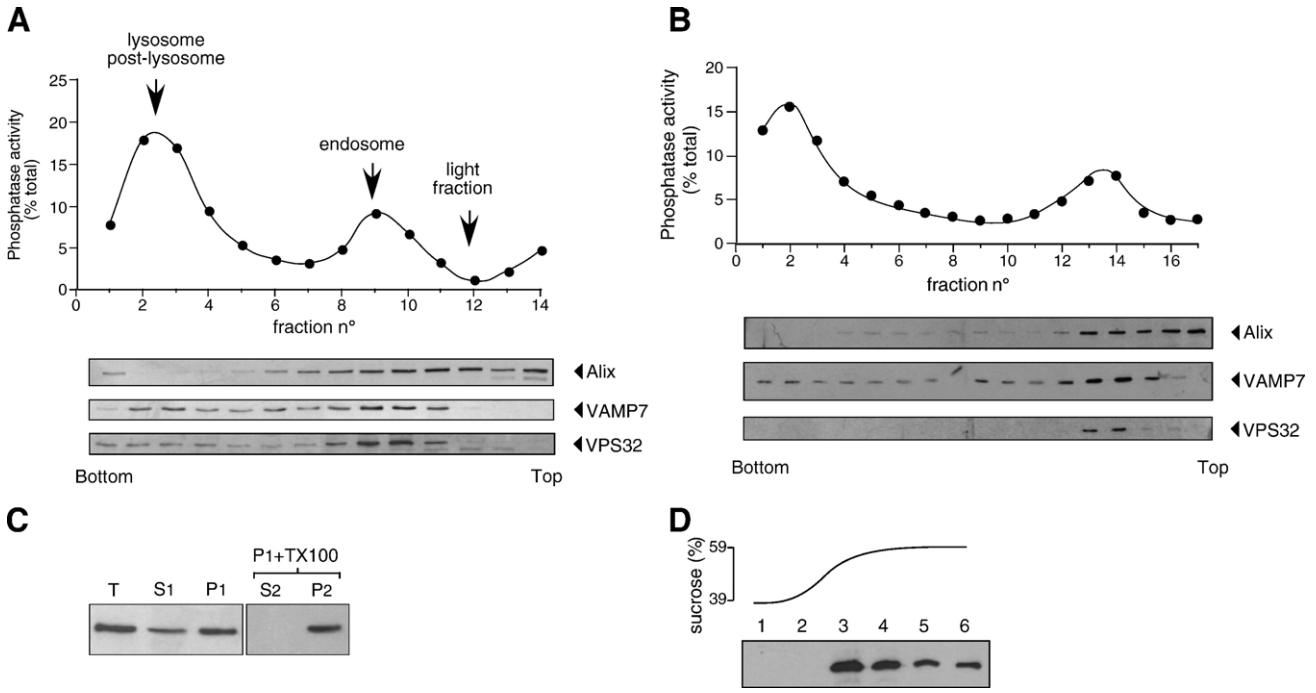

Fig. 7. Subcellular distribution of Dd-Alix. (A, B) Percoll gradient analysis. Postnuclear fractions (3 ml) from KAx-3 cells (A, vegetative; B, aggregation stage) were fractionated on a 24% Percoll gradient (21 ml) in MESES buffer and eluted by 1.7 ml (A) or 1.4 ml (B) fractions. Fractions were assayed for the acid phosphatase activity (●). The localization of Dd-Alix, VAMP7, and Dd-Vps32 was assessed by Western blot using the respective antibodies. (C) Differential centrifugation. Subcellular fractionation was performed on KAx-3 cells to obtain membrane and soluble fractions followed or not by a treatment with Triton X-100. T: postnuclear supernatant, S1: 13,000 × *g* supernatant, P1: 13,000 × *g* pellet, S2: 100,000 × *g* supernatant of 1% Triton X-100 treated P1, P2: 100,000 × *g* pellet of Triton-treated P1. (D) Flotation sucrose gradient. The P2 pellet was resuspended in 1 ml of 60% sucrose in MESES buffer, overlaid with two 2-ml layers of 55% and 35% sucrose in MESES buffer and spun for 18 h at 55,000 rpm in an SW65 rotor. Fractions were collected by 850 μl and tested for Alix presence by Western blot.

ment (dense fractions 2 to 4 positive for VAMP7 and acid phosphatase). Noticeably, a significant amount of the protein was found in a light fraction (tube 12). This compartment is poorly equipped with acid phosphatase and VAMP7 and its relatedness to the endocytic pathway is unclear. In developed cells, the proportion of membrane-associated Dd-Alix in the endosomal fractions (tubes 13–14) was increased (Fig. 7B). This enrichment may explain the changes observed by immunofluorescence as cells were shifted from nutritive status to starvation. Unfortunately, our anti-VAMP7 antibody was not good enough to assess the decoration of the endocytic compartments by both Alix and VAMP7 using immunofluorescence approaches.

To further analyze the membrane association of Dd-Alix, *Dictyostelium* cell lysates were separated at 13 000 × *g* to obtain a supernatant fraction (S) and a heavy membrane pellet (P). Dd-Alix partitioned between the supernatant and the particulate fractions in agreement with the immunofluorescence and the Percoll gradient analysis (Fig. 7C). Interestingly, extraction of the pellet with 1% of the nonionic detergent Triton X-100 did not allow solubilization of Dd-Alix (Fig. 7C). Additionally, when this Triton X-100-resistant extract was subjected to flotation in a sucrose density gradient, Dd-Alix partially floated up to the 35–55% sucrose interface, a behavior compatible with an association with lipid rafts (Fig. 7D).

Dd-Alix partially co-localizes with Dd-Vps32

Recently, several groups have described the interaction of Alix homologs with Vps32 (Katoh et al., 2003; Odorizzi et al., 2003; Strack et al., 2003; von Schwedler et al., 2003). Vps32 is part of a multiprotein complex ESCRT III involved with ESCRT I and II in the biogenesis of the MVB. In yeast, deletion of Vps32 or any member of the complex is associated with the formation of an abnormal compartment devoid of intralumenal vesicles, the class E compartment (Katzmann et al., 2002). The sequence of a *Dictyostelium* homolog of Vps32 was present in the Genbank database under the accession number AC116960.2. In this paper, we refer to this gene as *Dd-vps32*. It encodes a protein of 215 amino acids that shares 31% identity with its yeast homolog Vps32/Snf7 and 34–37% identity with the human isoforms CHMP4-a, b, and c. As observed for its yeast and human counterparts, Dd-Vps32 sequence contains several coiled-coil motifs and displays a heterogeneous distribution of the charged amino acids that results in a basic N-terminal part (aa 1 to 117, pI ~ 10) and an acidic C-terminal part (aa 118 to 215, pI ~ 4). In Western blot analysis, the anti-Vps32 antiserum recognized a single polypeptide with an apparent Mr of ~30 kDa instead of the 25 kDa expected from the calculated Mr, a difference also observed for its homologs (Babst et al., 2002a) and probably due to the high

percentage (around 35%) of charged amino acids. The behavior of Dd-Vps32 in subcellular fractionation assays was very similar to that of Dd-Alix, with part of the protein being associated with a Triton X-100-insoluble fraction (unpublished data). Despite the presence of a cocktail of protease inhibitors, the soluble Vps32 was highly sensitive to proteolysis. On a Percoll gradient of a vegetative, post-nuclear supernatant, the distribution of endogenous Dd-Vps32 essentially mimicked that of VAMP7. Dd-Vps32 overlapped with Dd-Alix at the level of the endosomal peak, but was excluded from the light fraction (Figs. 7A, B). As already observed for Dd-Alix, development was accompanied by an enrichment of Vps32 on the endosomal peak. The anti-Vps32 antibody was used to check whether Dd-Vps32 co-localized with Alix by immunofluorescence microscopy. In vegetative *alx* null cells expressing $Alix_{myc2}$, detection of Dd-Vps32 was very difficult and barely emerged from the non-specific background. On the other hand, in developed cells, endogenous Dd-Vps32 associated with small-sized vesicles scattered within the cytoplasm. Most of these vesicles were also positive for Dd-Alix staining, as indicated in the overlay (Fig. 8A). A few vesicles were positive, either for Dd-Alix only (closed arrow-heads) or Dd-Vps32 only (open arrow-heads). A C-terminally myc-tagged version of Dd-Vps32, $Vps32_{myc2}$, was overexpressed in KAx-3 and *alx* null cells under the constitutive *act15* promoter. Immunofluorescence analysis of KAx-3 cells using either the anti-myc or the anti-Vps32 antibody showed a clear pattern for Dd-Vps32 immunostaining. Though $Vps32_{myc2}$ associated to vesicular structures, heterogeneity in size and number could be observed, both in vegetative and developed cells. Remarkably, some cells harbored a single vesicle as large as 1–2 μm in diameter accompanied or not by smaller ones (Fig. 8B). As shown on a higher magnification of such large vesicles (Fig. 8B HM), the anti-myc antibody decorated the membrane of the vesicle and was excluded from the lumen of the structure. In this strain, Dd-Alix co-localized with Dd-Vps32 on the large vesicular structures (Fig. 8C). Interestingly, a similar $Vps32_{myc2}$ immunostaining pattern was observed in the *alx* null background, suggesting that vesicular recruitment of Dd-Vps32 is not dependent upon Dd-Alix. Several hypotheses may explain the immunofluorescence pattern of $Vps32_{myc2}$ in the overexpressor strain compared to the parental strain: (1) Overexpression of $Vps32_{myc2}$ (2- to 3-fold over the endogenous level) enhanced the signal to noise ratio and the detection of pre-existing structures poorly stained in parental strain was now possible, even under vegetative conditions; 92) the vesicular association of Dd-Vps32 might be a kinetically rapid event and overexpression could favor the on-phase of the association and hence its observation; (3) overexpression of $Vps32_{myc2}$ induced the formation of a new compartment (E class-like). In any case, the heterogeneity of the vesicle size could be attributed either to a heterogeneous expression level of $Vps32_{myc2}$ or to the visualization of sequential steps in the formation of the large compartment. As the same images were also obtained with the non-tagged Dd-Vps32 construct (unpublished data), the possibility of a dominant-negative effect due to the myc tag was eliminated. How this particular compartment integrates into *Dictyostelium* endocytic apparatus is not known and whether it belongs to the fluid-phase bulk transiting pathway is not clear either. However, it is interesting to note that overexpression of $Vps32_{myc2}$ hardly affected the macropinocytic activity (unpublished data).

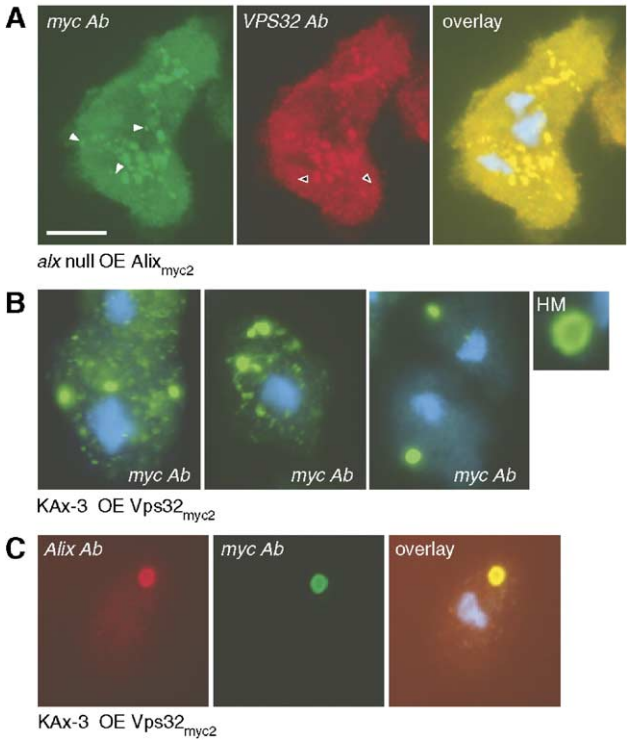

Fig. 8. Vesicular colocalization of Dd-Vps32 and Dd-Alix. (A) *alx* null cells expressing $Alix_{myc2}$ were let to develop overnight in Na-KP_i buffer on Labtek slides. Dd-Alix was stained with the anti-myc 9E10 antibody and a FITC-labeled secondary goat anti-mouse antibody. Dd-Vps32 was stained with the anti-Vps32 antibody and a Cy3-conjugated goat anti-rabbit antibody. In the overlay, most of the vesicles appeared yellow, an indication of colocalization of the two proteins. Some vesicles immunostained only by the anti-Alix antibody are indicated by closed arrowheads and vesicles positive only for Dd-Vps32 are indicated by open arrowheads. (B) KAx-3 cells overexpressing $Vps32_{myc2}$ were stained with the anti-Dd-Vps32 antibody and with DAPI to label the nucleus. Dd-Vps32 distribution varied intercellularly with cells harboring large and small vesicles (40%), cells with intermediate vesicles (35%) and cells with a single large vesicle with a 1- to 2-m diameter (25%). The photographs represent an overall view of the staining diversity. One large vesicle is presented at a higher magnification (HM) to show that Dd-Vps32 labeling is restricted to the membrane of the vesicle. C) In KAx-3 cells overexpressing $Vps32_{myc2}$, Dd-Alix labeled with the anti-Alix antibody co-localized with $Vps32_{myc2}$ on the larger vesicles. Cells were observed on a Zeiss Axiovert 200M microscope. Scale bars denote 5 μm.

Alix deletion leads to a modified cell surface protein profile

In yeast, Alix homolog Bro1 functions in MVB biogenesis and its deletion affects trafficking of the cell surface

permease GAP1 (Nikko et al., 2003). As Dd-Alix is also associated with the endocytic apparatus, we wondered whether the *alx* null strain had a defect in membrane protein trafficking and therefore harbored a different cell surface protein profile compared to the parental strain. To address this issue, we followed a general approach consisting of labeling the cell surface proteins with an analog of biotin and comparing the biotinylation pattern of both strains at different times of development. To avoid the morphogenesis steps that could interfere with labeling because of the tight aggregation of the cells, cells were developed in suspension by addition of exogenous cAMP. After a 4-h period of pulses with 30 nM cAMP, conditions that mimic the aggregation phase, cells were stimulated with high cAMP concentration to induce differentiation. Most of the pattern of biotinylated proteins was similar in the parental and *alx* null cells (Fig. 9). Nevertheless, at least three proteins showed significant differences between the two strains (Fig. 9, bands a, b, and c). In all cases, these proteins reacted strongly with streptavidin in the null cells when they were hardly visible in the parental cells. The quantitative differences in the cell surface protein profile between the two strains could result from a reduction of their rate of degradation thus supporting a role for Alix in plasma membrane protein transit. However, we cannot exclude the possibility that deletion of Alix affects the level of expression of these plasma membrane proteins.

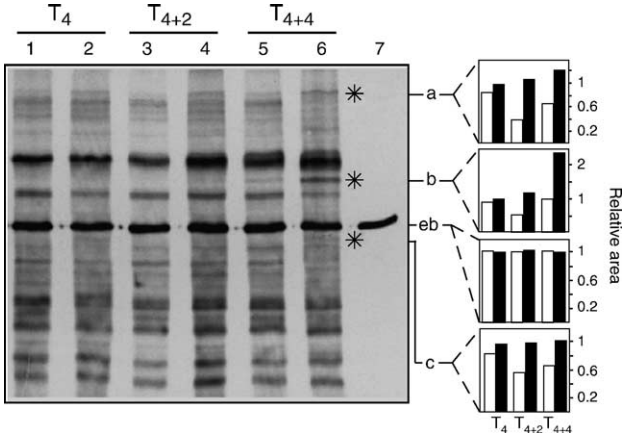

Fig. 9. Residence of some plasma membrane proteins is modified in *alx* null mutant. Cells were resuspended in starvation buffer and pulsed for 4 h with 30 nM cAMP (t4). After the pulsing period (t4), cells were maintained in the same medium and further stimulated by addition of 300 μM cAMP every 2 h. At times t4, t4 + 2, t4 + 4, cells were harvested and labeled with sulfo-NHS-LC-biotin for 15 min on ice. After quenching and washes, cells were lysed in Laemmli buffer and the pattern of biotinylation analyzed by SDS-PAGE and ECL using streptavidin-HRP to detect the biotin. The equivalent of 3×10^4 cells was loaded per lane. Lane 1, 3, 5: JH10; lane 2, 4, 6: *alx* null; lane 7, unlabelled *alx* null cell lysate. Lane 7 reveals an endogenously-biotinylated 80 kDa protein (Gotthardt et al., 2002). Signals corresponding to bands a, b, c were integrated over the whole lane using ImageJ program. The endogenously-biotinylated protein (eb) was used as a loading control. Results are presented as histograms for the different development conditions and for parental stain (gray columns) and *alx* null mutant (black columns).

Discussion

We report here the characterization of *Dictyostelium* Alix as the functional homolog of mammalian protein Alix. This protein is also present in *Saccharomyces cerevisiae* (Bro1), *Drosophila melanogaster*, *Xenopus laevis* (Xp95), and *Caenorhabditis elegans* (YNK1). Like its counterparts, Dd-Alix is composed of an N-terminal region, containing the Bro1 signature, a coiled-coil domain and a C-terminal polyproline-rich domain (PRD).

In order to dissect the role of Dd-Alix, we constructed a knock-out strain and analyzed the effect of *Dd-alx* deletion. Besides a unicellular growing phase, the *Dictyostelium* developmental cycle includes a multicellular phase that associates both differentiation/programmed cell death and morphogenetic processes. Abrogation of Alix function in *Dictyostelium* did not cause any measurable defect in various cellular parameters of the vegetative phase including growth, macropinocytosis, and phagocytosis of bacteria. A major impairment was detected during the developmental phase as the Dd-*alx* null cells failed to undergo morphogenesis and proper cell-type differentiation, defects that seriously compromised the formation of mature fruiting bodies. Whereas most cells (about 80%) engage in the prespore differentiation pathway in the parental strain, the *alx* null mutant preferentially differentiates prestalk cells at the expense of the prespore population. As a result, the multicellular structure that forms is devoid of spore cells. Dd-Alix is thus required for multicellular development and appropriate morphogenesis. Analysis of chimeric organisms indicates a cell-autonomous requirement of Dd-Alix for prespore differentiation. Additionally, though *alx* null cells preferentially adopt a prestalk fate, they fail to distribute homogeneously within the prestalk-derived structures when mixed with wild-type cells. This behavior has to be paralleled with the fact that the mutant cells express the ecmB marker early during differentiation and at a fairly high level compared to the ecmA marker, indicating that loss of Dd-Alix might favor a PstB fate. A requirement of Dd-Alix for appropriate prestalk and prespore cell differentiation is consistent with Dd-Alix being expressed in both cell types (SM, LA and GK, unpublished data). In *Dictyostelium*, the prestalk cells follow a programmed cell death process that leads to the formation of enlarged vacuolated dead stalk cells (Levraud et al., 2003). The presence of vacuolated stalk cells in the null mutant suggests that if Dd-Alix is involved in cell death as described in mammals, it does not function as an executioner in stalk cell death. During the course of this work, the group of Maki (Ohkouchi et al., 2004) reported the disruption of Dd-Alix in the Ax2 strain. The resulting phenotype is perceivable only under low Ca^{2+} conditions. In our hands, increasing the calcium concentration to 1 mM did not restore a parental phenotype. A different strain-sensitivity to Ca^{2+} variations may therefore explain the discrepancy between the results. A role for calcium signaling in the Alix pathway was indeed expected

from the calcium-dependent interaction of Dd-Alix with the calciproteins ALG-2a and ALG-2b (SM, LA, and GK unpublished data). However, we have shown previously that neither ALG-2a nor ALG-2b is essential for multicellular development (Aubry et al., 2002). This does not exclude the possibility that other partners of Dd-Alix may mediate the calcium effects.

In an effort to approach the function of Dd-Alix, we investigated the subcellular distribution of the protein. Besides a soluble pool, part of Dd-Alix resides on vesicles that probably derive from the endocytic apparatus. In this respect, *Dictyostelium* is similar to the macrophage, where Alix has been identified on latex bead-containing phagosomes (Garin et al., 2001) and to yeast, in which Bro1 associates with endosomes in the multivesicular body formation pathway (Odorizzi et al., 2003). As cells proceed throughout development, translocation onto vesicles is enhanced. It is therefore tempting to attribute the developmental function of Dd-Alix to the vesicular pool. The Alix-positive vesicles also carry the homolog of the endocytic protein Vps32, Dd-Vps32 characterized herein. Colocalization of Dd-Alix and Dd-Vps32 was foreseeable from yeast 2-hybrid data on mammalian Alix (Sadoul, unpublished data) and confirmed during the course of this work in yeast and mammals (Katoh et al., 2003; Odorizzi et al., 2003; Strack et al., 2003; von Schwedler et al., 2003). Attempts to demonstrate a direct interaction between Dd-Alix and Dd-Vps32 were unsuccessful due to their association with Triton X-100-insoluble fractions. In yeast, Vps32 participates in the biogenesis of the MVB. The MVB is a pre-lysosomal intermediate compartment that carries on intralumenal vesicles membrane proteins/receptors due to degradation. Vps32 belongs to the MVB sorting machinery that drives the clustering of the receptors in the invaginating vesicles and the invagination process itself (Gruenberg and Stenmark, 2004; Katzmann et al., 2002). Through a combination of genetic and biochemical approaches, the group of Emr has broken down the yeast sorting machinery into three subcomplexes, ESCRT-I (Katzmann et al., 2001), ESCRT-II (Babst et al., 2002b) and ESCRT-III that includes Vps32 (Babst et al., 2002a). Homologs of their components have been identified in human and our gene mining of *Dictyostelium* genome gave highly probable hits for all components: for ESCRT-I, Vps23/Tsg101 (DDB0187043), Vps28 (DDB0186436) and Vps37 (DDB0190314); for ESCRT-II, Vps22 (DDB0185415), Vps25 (DDB0189483) and Vps36 (DDB0213300); for ESCRT-III, Vps2 (DDB0188723), Vps20 (DDB0187234), Vps24 (DDB0189855) and Vps32 (3 isoforms: DdVps32, DDB0187725 and DDB0169062) and for the ESCRT complex-dissociating AAA-ATPase Vps4 (DDB0185960) (http://dictybase.org, Kreppel et al., 2004). The ESCRT machinery is therefore evolutionarily conserved and it is likely that the ESCRT complexes come into play during the developmental functioning of Dd-Alix to downregulate specific cell surface receptors. Membrane association of the ESCRT components is dynamic and the off-step is mediated by the ATP-hydrolyzing activity of Vps4. How their recruitment onto the membrane is regulated is obscure. Nevertheless, our data based on the use of the *alx* null strain clearly demonstrate that Dd-Vps32 vesicular association is not dependent on the presence of Dd-Alix. Overexpression of $Vps32_{myc2}$ is accompanied by a new pattern of distribution of the protein on vesicles highly heterogeneous in size, the larger of which also harboring Dd-Alix. These large vesicles, up to several microns in diameter, are reminiscent of the class E compartment in yeast generated by Vps32 knock-out or dominant-negative Vps32 proteins (Howard et al., 2001). Even though the nature of the vesicles remains to be firmly established, the $Vps32_{myc2}$ overexpressor opens up new prospects as a tool to dissect Dd-Alix/ESCRT interplay.

Interaction of Alix with the ESCRT machinery is mediated in part by the N-terminal Bro1-containing domain (aa 1 to 423) which binds Vps32 via a yet undefined motif (Katoh et al., 2003; Martin-Serrano et al., 2003; Strack et al., 2003; von Schwedler et al., 2003) and the PRD which recruits Tsg101 through a PS/TAP sequence (von Schwedler et al., 2003). Deletion of the Bro1 domain of Dd-Alix yielded unstable proteins during the differentiation stage and therefore did not permit evaluation of the contribution of the Nt-domain to the function of the full-length protein. But clearly, this domain is not sufficient by itself to fulfill Dd-Alix developmental function as its overexpression failed to restore the parental phenotype. Interestingly, the N-terminal part of Alix that includes the integrality of the Bro1 domain plus the AQAQE sequence is present in rhophilins, where it functions together with the Rho-binding domain to disassemble F-actin stress fibers (Peck et al., 2002). Alix itself has been described to reduce phosphorylation of focal adhesion kinases (Schmidt et al., 2003) and could thereby locally modify the cytoskeletal network possibly via its N-terminal domain. Alix might function as a connector, at a given site of the forming MVB, between the sorting machinery and the mechanical network driving intralumenal vesicle invagination. We showed that the C-terminal PRD of Dd-Alix is dispensable for the rescue of the *alx* null strain development. In mammals, the PRD is essential for the binding of various partners including the adaptor SETA/Ruk (Chen et al., 2000), endophilins (Chatellard-Causse et al., 2002), ALG-2 (Missotten et al., 1999) in addition to Tsg101 (von Schwedler et al., 2003). Therefore, the ability of the AlixΔPro construct to rescue the null phenotype first raises the question of the requirement of the above interactions for Alix function in *Dictyostelium* and second, pinpoint the upstream coiled-coil containing region as essential for development. Interestingly, this coiled-coil domain has recently been shown as essential for MVB sorting in yeast (Luhtala and Odorizzi, 2004). So far, we have been unable to identify partners of this domain in a yeast two-hybrid screen.

In *Dictyostelium*, the developmental program that is engaged upon starvation is dependent on a number of cell

surface receptors such as cAMP receptors (cARs) and the receptors for conditioned medium factor (CMFR). The selective internalization of cARs has been proposed as a mechanism to attenuate (Wang et al., 1988) and thereby restrict signaling to specific cell-types and/or steps of *Dictyostelium* development. In mammals, clathrin-dependent endocytosis has been particularly well-studied as the major route for internalization and recycling or degradation of cell-surface receptors. Deletion of *Dictyostelium* clathrin heavy chain (CHC) yields premature developmental arrest and an incorrect expression and downregulation of cARs (Niswonger and O'Halloran, 1997). It is probable that other developmental receptors are regulated in a clathrin-dependent manner. Interestingly, the developmental phenotype induced by *alx* null mutation is reminiscent of that seen with the clathrin heavy chain (*chc*)-null strain, an observation in strong support for Dd-Alix regulating membrane signaling molecules essential for development along an endocytic pathway. Consistently, deletion of Dd-Alix induces a change in the cell surface protein profile. Our results can be combined in the following model: during development, Alix cooperates with the ESCRT sorting machinery at the level of the MVB (or its equivalent in *Dictyostelium*) to attenuate signaling pathways by downregulation of the upstream receptors in a temporally and/or spatially-dependent manner. In the *alx* knock-out strain, persistence of these receptors at the plasma membrane would lead to a prolonged signaling and conflicting downstream cascades resulting in the observed phenotype. Because of the major defect in the prespore differentiation pathway, we favor a cell-type specific receptor as target. Ongoing studies based on the systematic and comparative analysis of the behavior of specific candidates, both in the *alx* null mutant and in the parental strain, should help to identify the target(s) in *Dictyostelium*. In addition, among the collection of *Dictyostelium* developmental mutants, several share phenotypic similarities with the *alx* null mutant. The strain disrupted in TipC (Stege et al., 1999), a homologue of the yeast Vps13 implicated in the trafficking of proteins from the *trans*-Golgi network and endosome to the vacuole, is representative of that category of mutants. Altogether, they represent valuable tools to pinpoint potential partners of the Alix pathway.

Acknowledgments

This work was supported in part by the Commissariat à l'Energie Atomique, the Centre National de la Recherche Scientifique, the Université Joseph Fourier Grenoble, the Ministère pour la Recherche et la Technologie (ACI Biologie du Développement et Physiologie Intégrative) and by grants from the Association pour la Recherche sur le Cancer (ARECA/Biologie Structurale du Cancer). The authors would like to thank Pierre Golstein and his group for constructive and stimulating discussions, Rick Firtel for generously providing cell lines and expression vectors and Franz Bruckert for the gift of anti-VAMP7 antibody. The sequencing and the analysis of the genome of *Dictyostelium discoideum* is an international collaboration between the University of Cologne, Germany, the Institute of Molecular Biotechnology in Jena, Germany, the Baylor College of Medicine in Houston, USA, Medical Research Council Laboratory of Molecular Biology, University of Dundee, UK, the Pasteur Institute in Paris, France, and the Sanger Centre in Hinxton, UK.

References

Aubry, L., Firtel, R., 1999. Integration of signaling networks that regulate *Dictyostelium* differentiation. Annu. Rev. Cell Dev. Biol. 15, 469–517.

Aubry, L., Mattei, S., Blot, B., Sadoul, R., Satre, M., Klein, G., 2002. Biochemical characterization of two analogues of the apoptosis-linked gene 2 protein in *Dictyostelium discoideum* and interaction with a physiological partner in mammals, murine Alix. J. Biol. Chem. 277, 21947–21954.

Babst, M., Katzmann, D.J., Estepa-Sabal, E.J., Meerloo, T., Emr, S.D., 2002a. ESCRT-III: an endosome-associated heterooligomeric protein complex required for MVB sorting. Dev. Cell 3, 271–282.

Babst, M., Katzmann, D.J., Snyder, W.B., Wendland, B., Emr, S.D., 2002b. Endosome-associated complex, ESCRT-II, recruits transport machinery for protein sorting at the multivesicular body. Dev. Cell 3, 283–289.

Chatellard-Causse, C., Blot, B., Cristina, N., Torch, S., Missotten, M., Sadoul, R., 2002. Alix (ALG-2-interacting protein X), a protein involved in apoptosis, binds to endophilins and induces cytoplasmic vacuolization. J. Biol. Chem. 277, 29108–29115.

Chen, B., Borinstein, S.C., Gillis, J., Sykes, V.W., Bögler, O., 2000. The glioma-associated protein SETA interacts with AIP1/Alix and ALG-2 and modulates apoptosis in astrocytes. J. Biol. Chem. 275, 19275–19281.

Early, A., Abe, T., Williams, J., 1995. Evidence for positional differentiation of prestalk cells and for a morphogenetic gradient in *Dictyostelium*. Cell 83, 91–99.

Garin, J., Diez, R., Kieffer, S., Dermine, J.F., Duclos, S., Gagnon, E., Sadoul, R., Rondeau, C., Desjardins, M., 2001. The phagosome proteome: insight into phagosome functions. J. Cell Biol. 152, 165–180.

Glöckner, G., Eichinger, L., Szafranski, K., Pachebat, J.A., Bankier, A.T., Dear, P.H., Lehmann, R., Baumgart, C., Parra, G., Abril, J.F., Guigo, R., Kumpf, K., Tunggal, B., Cox, E., Quail, M.A., Platzer, M., Rosenthal, A., Noegel, A.A., 2002. Sequence and analysis of chromosome 2 of *Dictyostelium discoideum*. Nature 418, 79–85.

Golstein, P., Aubry, L., Levraud, J.P., 2003. Cell-death alternative model organisms: why and which? Nat. Rev. Mol. Cell. Biol. 4, 798–807.

Gotthardt, D., Warnatz, H.J., Henschel, O., Bruckert, F., Schleicher, M., Soldati, T., 2002. High-resolution dissection of phagosome maturation reveals distinct membrane trafficking phases. Mol. Biol. Cell 13, 3508–3520.

Gruenberg, J., Stenmark, H., 2004. The biogenesis of multivesicular endosomes. Nat. Rev., Mol. Cell. Biol. 5, 317–323.

Haberstroh, L., Firtel, R.A., 1990. A spatial gradient of expression of a cAMP-regulated prespore cell type-specific gene in *Dictyostelium*. Genes Devel. 4, 596–612.

Harlow, E., Lane, D., 1988. Antibodies. A Laboratory Manual. Cold Spring Harbor Laboratory, New York.

Harrington, B.J., Raper, K.B., 1968. Use of a fluorescent brightener to demonstrate cellulose in the cellular slime mold. J. Appl. Microbiol. 16, 106–113.

Howard, T.L., Stauffer, D.R., Degnin, C.R., Hollenberg, S.M., 2001. CHMP1 functions as a member of a newly defined family of vesicle trafficking proteins. J. Cell Sci. 114, 2395–2404.

Jermyn, K.A., Duffy, K.T., Williams, J.G., 1989. A new anatomy of the prestalk zone in *Dictyostelium*. Nature 340, 144–146.

Katoh, K., Shibata, H., Suzuki, H., Nara, A., Ishidoh, K., Kominami, E., Yoshimori, T., Maki, M., 2003. The ALG-2-interacting protein Alix associates with CHMP4b, a human homologue of yeast Snf7 that is involved in multivesicular body sorting. J. Biol. Chem. 278, 39104–39113.

Katzmann, D.J., Babst, M., Emr, S.D., 2001. Ubiquitin-dependent sorting into the multivesicular body pathway requires the function of a conserved endosomal protein sorting complex ESCRT-I. Cell 106, 145–155.

Katzmann, D.J., Odorizzi, G., Emr, S.D., 2002. Receptor downregulation and multivesicular-body sorting. Nat. Rev., Mol. Cell Biol. 3, 893–905.

Kay, R.R., Jermyn, K.A., 1983. A possible morphogen controlling differentiation in *Dictyostelium*. Nature 303, 242–244.

Kreppel, L., Fey, P., Gaudet, P., Just, E., Kibbe, W.A., Chisholm, R.L., Kimmel, A.R., 2004. dictyBase: a new *Dictyostelium discoideum* genome database. Nucleic Acids Res. 32, D332–D333.

Levraud, J.P., Adam, M., Luciani, M.F., de Chastellier, C., Blanton, R.L., Golstein, P., 2003. *Dictyostelium* cell death: early emergence and demise of highly polarized paddle cells. J. Cell Biol. 160, 1105–1114.

Luhtala, N., Odorizzi, G., 2004. Bro1 coordinates deubiquitination in the multivesicular body pathway by recruiting Doa4 to endosomes. J. Cell Biol. 166, 717–729.

Maniak, M., 2001. Fluid-phase uptake and transit in axenic *Dictyostelium* cells. Biochim. Biophys. Acta 1525, 197–204.

Mann, S.K.O., Devreotes, P.N., Eliott, S., Jermyn, K., Kospa, A., Fechheimer, M., Furukawa, R., Parent, C.A., Segall, J., Shaulsky, G., Vardy, P.H., Williams, J., Williams, K.L., Firtel, R.A., 1994. Cell biological, molecular genetic, and biochemical methods to examin *Dictyostelium*. In: Celis, J.E. (Ed.), *Cell Biology*—A Laboratory Handbook. Academic Press, San Diego, pp. 412–451.

Martin-Serrano, J., Yaravoy, A., Perez-Caballero, D., Bieniasz, P.D., 2003. Divergent retroviral late-budding domains recruit vacuolor protein sorting factors by using alternative adaptor proteins. Proc. Natl. Acad. Sci. USA 100, 12414–12419.

Matsuo, H., Chevallier, J., Mayran, N., Le Blanc, I., Ferguson, C., Faure, J., Blanc, N.S., Matile, S., Dubochet, J., Sadoul, R., Parton, R.G., Vilbois, F., Gruenberg, J., 2004. Role of LBPA and Alix in multivesicular liposome formation and endosome organization. Science 303, 531–534.

Missotten, M., Nichols, A., Rieger, K., Sadoul, R., 1999. Alix, a novel mouse protein undergoing calcium-dependent interaction with the apoptosis-linked-gene 2 (ALG-2) protein. Cell Death Differ. 6, 124–129.

Nickas, M.E., Yaffe, M.P., 1996. BRO1, a novel gene that interacts with components of the Pkc1p-mitogen-activated protein kinase pathway in *Saccharomyces cerevisiae*. Mol. Cell. Biol. 16, 2585–2593.

Nikko, E., Marini, A.-M., André, B., 2003. Permease recycling and ubiquitination status reveal a particular role for Bro1 in the multivesicular body pathway. J. Biol. Chem. 278, 50732–50743.

Niswonger, M.L., O'Halloran, T.J., 1997. Clathrin heavy chain is required for spore cell but not stalk cell differentiation in *Dictyostelium discoideum*. Development 124, 443–451.

Odorizzi, G., Katzmann, D.J., Babst, M., Audhya, A., Emr, S.D., 2003. Bro1 is an endosome-associated protein that functions in the MVB pathway in *Saccharomyces cerevisiae*. J. Cell Sci. 116, 1893–1903.

Ohkouchi, S., El-Halawany, M.S., Aruga, F., Shibata, H., Hitomi, K., Maki, M., 2004. DdAlix, an Alix/AIP1 homolog in *Dictyostelium discoideum*, is required for multicellular development under low Ca2+ conditions. Gene 337, 131–139.

Peck, J.W., Oberst, M., Bouker, K.B., Bowden, E., Burbelo, P.D., 2002. The RhoA-binding protein, Rhophilin-2, regulates actin cytoskeleton organization. J. Biol. Chem. 277, 43924–43932.

Roisin-Bouffay, C., Luciani, M.F., Klein, G., Levraud, J.P., Adam, M., Golstein, P., 2004. Developmental cell death in *Dictyostelium* does not require paracaspase. J. Biol. Chem. 279, 11489–11494.

Ryves, W.J., Fryer, L., Dale, T., Harwood, A.J., 1998. An assay for glycogen synthase kinase 3 (GSK-3) for use in crude cell extracts. Anal. Biochem. 264, 124–127.

Schmidt, M.H., Chen, B., Randazzo, L.M., Bögler, O., 2003. SETA/CIN85/Ruk and its binding partner AIP1 associate with diverse cytoskeletal elements, including FAKs, and modulate cell adhesion. J. Cell Sci. 116, 2845–2855.

Sperandio, S., Poksay, K., De Belle, I., Lafuente, M.J., Liu, B., Nasir, J., Bredesen, D.E., 2004. Paraptosis: mediation by MAP kinases and inhibition by AIP-1/Alix. Cell Death Differ. 11, 1066–1075.

Springael, J.-Y., Nikko, E., André, B., Marini, A.-M., 2002. Yeast Npi3/Bro1 is involved in ubiquitin-dependent control of permease trafficking. FEBS Lett. 517, 103–109.

Stege, J.T., Laub, M.T., Loomis, W.F., 1999. tip genes act in parallel pathways of early *Dictyostelium* development. Dev. Genet. 25, 64–77.

Strack, B., Calistri, A., Craig, S., Popova, E., Göttlinger, H.G., 2003. AIP1/ALIX is a binding partner for HIV-1 p6 and EIAV p9 functioning in virus budding. Cell 114, 689–699.

Thompson, J.D., Higgins, D.G., Gibson, T.J., 1994. CLUSTAL W: improving the sensitivity of progressive multiple sequence alignment through sequence weighting, position-specific gap penalties and weight matrix choice. Nucleic Acids Res. 22, 4673–4680.

Town, C.D., Gross, J.D., Kay, R.R., 1976. Cell differentiation without morphogenesis in *Dictyostelium discoideum*. Nature 262, 717–719.

Trioulier, Y., Torch, S., Blot, B., Cristina, N., Chatellard-Causse, C., Verna, J.-M., Sadoul, R., 2004. Alix, a protein regulating endosomal trafficking, is involved in neuronal death. J. Biol. Chem. 279, 2046–2052.

Vincent, O., Rainbow, L., Tilburn, J., Arst, H.N.J., Penalva, M.A., 2003. YPXL/I is a protein interaction motif recognized by Aspergillus PalA and its human homologue, AIP1/Alix. Mol. Cell. Biol. 23, 1647–1655.

Vito, P., Pellegrini, L., Guiet, C., D'Adamio, L., 1999. Cloning of AIP1, a novel protein that associates with the apoptosis-linked gene ALG-2 in a Ca2+-dependent reaction. J. Biol. Chem. 274, 1533–1540.

von Schwedler, U.K., Stuchell, M., Muller, B., Ward, D.M., Chung, H.Y., Morita, E., Wang, H.E., Davis, T., He, G.P., Cimbora, D.M., Scott, A., Krausslich, H.G., Kaplan, J., Morham, S.G., Sundquist, W.I., 2003. The protein network of HIV budding. Cell 114, 701–713.

Wang, M., Van Haastert, P.J., Devreotes, P.N., Schaap, P., 1988. Localization of chemoattractant receptors on *Dictyostelium* discoideum cells during aggregation and down-regulation. Dev. Biol. 128, 72–77.

Williams, J.G., Duffy, K.T., Lane, D.P., McRobbie, S.J., Harwood, A.J., Traynor, D., Kay, R.R., Jermyn, K.A., 1989. Origins of the prestalk-prespore pattern in *Dictyostelium* development. Cell 59, 1157–1163.

Wu, Y., Pan, S., Luo, W., Lin, S.-H., Kuang, J., 2002. Hp95 promotes anoikis and inhibits tumorigenicity of HeLa cells. Oncogene 21, 6801–6808.